Chinese Chemical Letters 34 (2023) 108617

Contents lists available at ScienceDirect

Chinese Chemical Letters

journal homepage: www.elsevier.com/locate/cclet

An amphiphilic molecule with a single fluorophore exhibits multiple stimuli-responsive behavior ☆

Dongxing Ren[a], Lu Tang[a], Zhiying Wu[a], Qiaona Zhang[a], Tangxin Xiao[a,*], Robert B.P. Elmes[b], Leyong Wang[c]

[a] School of Petrochemical Engineering, Changzhou University, Changzhou 213164, China
[b] Department of Chemistry, Maynooth University, National University of Ireland, Maynooth, Co. Kildare, Ireland
[c] Jiangsu Key Laboratory of Advanced Organic Materials, School of Chemistry and Chemical Engineering, Nanjing University, Nanjing 210023, China

ARTICLE INFO

Article history:
Received 24 March 2023
Revised 19 May 2023
Accepted 24 May 2023
Available online 26 May 2023

Keywords:
Self-assembly
Multi-responsive fluorescence
Single fluorophore
Information encryption
Smart materials

ABSTRACT

Fluorescent materials that respond to multiple stimuli have broad applications ranging from sensing and bioimaging to information encryption. Herein, we report the design and synthesis of a single-fluorophore-based amphiphile **DCSO**, which shows temperature-, solvent-, humidity-, and radiation-dependent fluorescence. **DCSO** consists of a dicyanostilbene (DCS) group as a rigid hydrophobic core with oligo(ethylene glycol) (OEG) chains at both ends as a flexible hydrophilic periphery. The DCS group acts as a highly efficient fluorophore, while the OEG chain endows the molecule with thermo-responsiveness. Fluorescent colors can vary from blue to green to yellow in response to external stimuli. On the basis of light radiation, we demonstrate that this system can be applied to time-dependent information encryption, in which the correct information can only be read at a specific time under irradiation. This work further demonstrates the usefulness and application of single-fluorophore-based luminescent materials with multiple stimuli-responsive functions.

Nature displays many examples of organisms that display functional responses to environmental changes [1]. For example, chameleons have the remarkable ability to camouflage themselves by changing their skin color depending on their environment [2,3]. Inspired by this, scientists have long pursued the advent of synthetic stimuli-responsive systems that respond to a specific signal to meet various real-life requirements [4–7]. In particular, optical signals are highly desirable due to several useful characteristics, such as rapid response times, high sensitivity, and instant visualization [8,9]. Changes in luminescence color or intensity in response to external stimuli can be used as ideal feedback to indicate the responsive behavior of the system. As a result, the field of stimuli-responsive luminescent materials has become an active area of research [10–16].

In this context, luminescent materials based on organic molecules are of particular interest due to their roles in many active fields of research. However, many of the reported systems only exhibit a fluorescence response to a single external stimulus [8,17], such as photo- [18], mechano- [19], thermo- [20,21], and solvatochromic signals [22]. In contrast, materials containing a single organic fluorophore that respond to multiple stimuli to elicit a change in fluorescence behavior are considerably more scarce – even though such systems are highly desirable [23–25].

Herein, we report **DCSO**, a multiple stimuli-responsive fluorescent system achieved by attaching oligo(ethylene glycol) (OEG) groups onto both sides of a dicyanostilbene (DCS) motif (Scheme 1). The OEG groups should enable the dissolution and self-assembly of the amphiphile in aqueous media while also being thermo-responsive in water due to the hydrophilic-to-hydrophobic change of the glycol chains upon heating [26–31]. For example, we recently developed a variety of thermo-responsive fluorescent materials mediated by OEG groups [32,33]. In this work, we show that **DCSO** not only exhibits thermo-responsive behavior, but also shows solvatochromic and humidity-responsive characteristics where the fluorescence color of the material exhibited dramatic spectral variation ranging from blue to yellow through green in response to the external stimuli. Most interestingly, the material also showed a time-dependent UV irradiation response in fluorescence, which was exploited for transient information storage and encryption [34].

DCSO was synthesized by an etherification reaction of a dihydroxy DCS-core with a benzyl bromide compound decorated

☆ This paper is dedicated to Professor Yu Liu on the occasion of his 70th birthday.

* Corresponding author.
E-mail address: xiaotangxin@cczu.edu.cn (T. Xiao).

https://doi.org/10.1016/j.cclet.2023.108617
1001-8417/

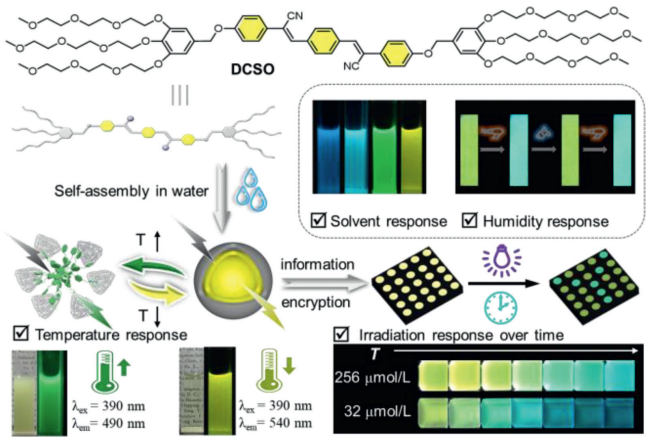

Scheme 1. Schematic illustration of the multiple stimuli-responsive fluorescence system based on a single fluorophore: the chemical structure of **DCSO** and its responsive behavior to temperature, solvent, humidity, and irradiation.

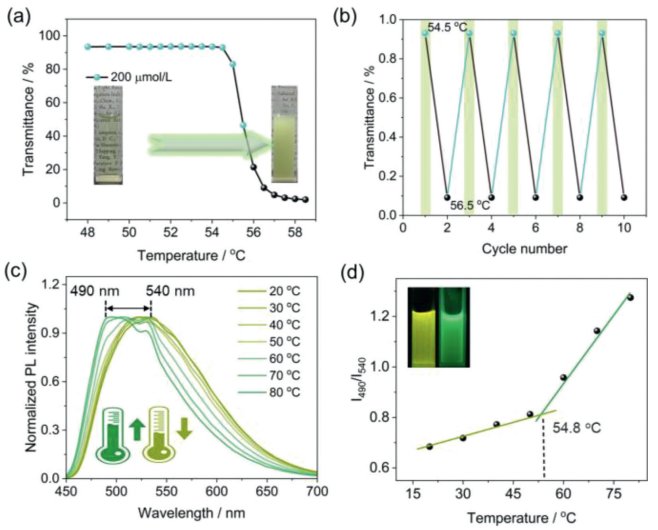

Fig. 1. Thermo-responsive behavior of **DCSO** and its temperature-dependent photophysical properties. (a) Temperature-dependent transmittance of **DCSO** at 500 nm in water, [**DCSO**] = 200 μmol/L, insets: photographs of the solution below and above T_{cloud}. (b) Reversible changes in optical transmittance of **DCSO** when cycling between 54.5 and 56.5 °C ([**DCSO**] = 200 μmol/L). (c) Temperature-dependent normalized PL spectra of **DCSO** in water ([**DCSO**] = 200 μmol/L, λ_{ex} = 390 nm). (d) Plot of fluorescence intensity ratio between 490 and 540 nm (I_{490}/I_{540}) as a function of temperature, insets: photographs of **DCSO** solution at 20 °C (left) and 80 °C (right).

with OEG chains (Scheme S1 and Figs. S1-S3 in Supporting information). Importantly, **DCSO** can be dissolved in both organic solvent and water. With **DCSO** in hand, we first investigated its concentration-dependent self-assembly behavior in water owing to its amphiphilic nature. Dilute solutions of **DCSO** are weakly emissive (Fig. S4 in Supporting Information), however, when the concentration was increased to 256 μmol/L, the photoluminescence (PL) intensity was significantly enhanced before reaching a plateau — verifying that **DCSO** is exhibiting aggregation-induced emission (AIE). This behavior also suggests that **DCSO** is completely dissolved in dilute solution exhibiting weak emission while it exists as nanoaggregates in higher concentration solutions, with the fluorophores packed closely together, resulting in a significant fluorescence enhancement. The critical aggregation concentration (CAC) of **DCSO** was measured to be 176 μmol/L by concentration-dependent full-wavelength optical transmittance (Fig. S5 in Supporting information). A clear Tyndall effect was observed in 200 μmol/L **DCSO** aqueous solution, indicating the presence of abundant nanoaggregates. The size of the nanoaggregates was subsequently measured by dynamic light scattering (DLS), exhibiting an average hydrodynamic diameter of *ca.* 41 nm (Fig. S6a in Supporting information). In order to further study the morphology of the nanoaggregates, transmission electron microscopy (TEM) was also carried out, and showed spherical nanoparticles with a diameter of about 20∼30 nm (Fig. S6b in Supporting information).

The lower critical solution temperature (LCST) behavior [31,35-37] of **DCSO** was further investigated. As shown in Fig. 1a, a transparent aqueous solution of **DCSO** (200 μmol/L) at 25 °C became turbid when heated to 56 °C. The cloud point temperature (T_{cloud}) of **DCSO** under these conditions was determined to be 55.5 °C by monitoring the temperature-dependent transmittance at 500 nm. The LCST behavior of **DCSO** is likely due to the dynamic interaction of OEG chains with surrounding water molecules. When $T_{test} < T_{cloud}$, OEG chains can form hydrogen bonded networks with water molecules, making **DCSO** amphiphilic and forming well-ordered nanoparticles, resulting in a transparent solution. However, when $T_{test} > T_{cloud}$, the hydrogen bonded networks will be disrupted by the high temperature, causing the OEG chains to become hydrophobic. As a result, the entire **DCSO** molecule loses its amphiphilicity, leading to phase separation and ultimately, a turbid solution. It is also worth noting that the LCST behavior of **DCSO** can be modulated by changing the concentration (Fig. S8 in Supporting information). T_{cloud} decreased from 59.9 °C to 52.5 °C when the concentration was increased from 50 μmol/L to 700 μmol/L. Fig. 1b shows the reversible phase transition of **DCSO** upon several heating/cooling cycles without any evidence of fatigue. This behavior verifies that **DCSO** displays outstanding temperature-responsiveness.

Given the LCST behavior of **DCSO**, we wondered whether **DCSO** would display temperature-dependent fluorescence characteristics owing to the different aggregation states between heating and cooling. Subsequently, a temperature-dependent fluorescence experiment was performed where the temperature was increased from 20 °C to 80 °C. Under these conditions the fluorescence maximum showed a significant blue-shift from 540 nm to 490 nm (Fig. 1c) which resulted in the fluorescence color changing from greenish yellow to green. In addition, with the increase of temperature, the fluorescence intensity of **DCSO** at 540 nm gradually decreased, while the emission peak at 490 nm gradually increased. This change can be represented by the relationship between I_{490}/I_{540} (I represents the PL intensity) and temperature (Fig. 1d). With the increase of temperature, an inflection point is observed at 54.8 °C, and aligns to the cloud point determined by fluorescence. This value is also consistent with the T_{cloud} (55.5 °C) measured by optical transmittance. In parallel, the absolute fluorescence quantum yield decreased from 19% at room temperature to 14% at high temperature (Fig. S14 in Supporting information). We expect that when the solution is at 20 °C, **DCSO** molecules are stacked together to form well-ordered nanospheres where the tight packing of the fluorophores restricts intramolecular motion and leads to strong emission intensity. Upon heating, however, a phase transition occurs where the tightly packed fluorophores begin to loosen (but remain aggregated) (Fig. S7 in Supporting information), resulting in a reduced fluorescence. To understand the observed blue shift, we further conducted a temperature-dependent UV-vis absorption study (Fig. S9 in Supporting information). When the temperature was increased to exceed 55.5 °C (T_{cloud}), the absorption between 340 and 420 nm significantly decreased and new absorption bands between 260 and 340 nm appeared, indicative of the formation of H-like aggregates. In contrast, **DCSO** in well-ordered nanospheres at 20 °C may exist as J-like aggregates (*vide infra*). Therefore, the blue shift in fluorescence may be due to the transformation of **DCSO** aggregation morphology upon heating.

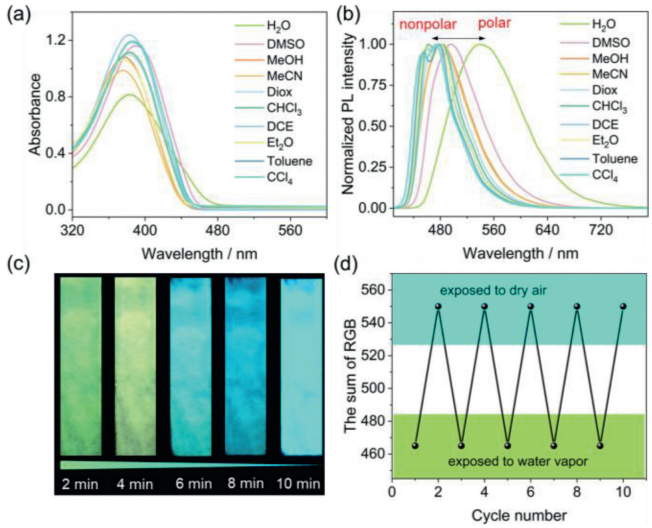

Fig. 2. Solvatochromic and humidity-responsive emission behaviors of **DCSO**. (a) UV-vis spectra of **DCSO** in various solvents (note: Diox = 1,4-dioxane, DCE = 1,2-dichloroethane). (b) Normalized emission spectra of **DCSO** in different solvents ([**DCSO**] =200 μmol/L, λ_{ex} = 390 nm). (c) Time-dependent photographs of wet **DCSO** films during drying under UV light. (d) Reversible changes in fluorescence color of the **DCSO** film in response to water vapor.

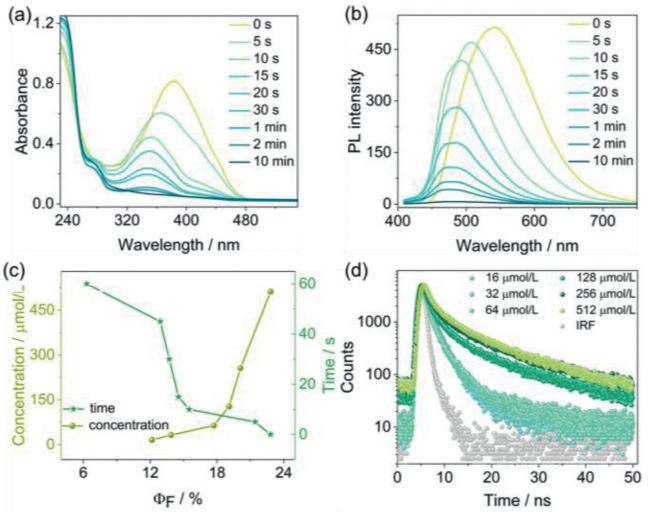

Fig. 3. Concentration- and time-dependent irradiation-responsive fluorescence of **DCSO** in water. (a) UV-vis absorption and (b) fluorescence spectra of **DCSO** at different UV light exposure times ([**DSCO**] = 200 μmol/L, λ_{irr} = 365 nm, λ_{ex} = 390 nm). (c) Absolute fluorescence quantum yields (Φ_F) of **DCSO** at different concentrations (before irradiation) and irradiation times ([**DCSO**] = 512 μmol/L). (d) Fluorescence decay profiles of **DCSO** at different concentrations.

Solvatochromic materials have gained considerable attention in recent years [38–41], thus, we also studied the photophysical properties of **DCSO** in different solvents. **DCSO** dissolves well in CH_3CN, leading to an absorption maximum at 374 nm. In contrast, the UV-vis spectrum of **DCSO** in H_2O exhibits significant differences as follows (Fig. 2a): (1) a red shift of absorption maximum to 385 nm, (2) the occurrence of a shoulder band at about 440 nm, (3) decreased absorption with concomitant band broadening. These observations suggest that a somewhat J-type aggregation had occurred in water. However, such an aggregation deviates from classical J-aggregates [42–44], as suggested by the wider absorption spectrum and the lower overall extinction coefficient. This is likely due to the abundance of rotating bonds in the DCS moiety and the large OEG chains prevent the formation of perfect J-aggregate stacks. Different fluorescence colors, ranging from yellow to green to blue, were observed in different solvents with reduced polarity (Fig. S10 in Supporting information), suggesting that **DCSO** may exhibit dual-state emission (DSE) [45,46] where fluorescence occurs in both aggregated and completely dissolved solution states. As shown in Fig. 2b, the emission spectrum exhibited a blue shift with decreasing solvent polarity. Specifically, with solvent polarity decreasing from water to CCl_4, the fluorescence maximum blue-shifted from 540 nm to 450 nm.

Given the unique fluorescent color of **DCSO** in water and the practical significance of humidity detection, the response of **DCSO** to water vapor when deposited on a filter paper was also studied. As shown in Fig. 2c, a wet film exhibits a greenish yellow fluorescence color but changed to bright cyan gradually over time. This cyan color in the dry state is similar to the fluorescent color observed in low polarity solvents and is likely due to the dielectric constant of air being close to that of low polarity solvents. Importantly, the color change between the wet and dry state can be repeated more than 10 times without obvious fatigue, indicative of excellent humidity-responsiveness (Fig. 2d).

As the cyanostilbene group is well-known for its photo-responsive behavior [39,47-49], the responsive properties of **DCSO** in water upon UV-irradiation were next investigated. As shown in Scheme 1, with increasing irradiation time (irradiation wavelength: λ_{irr} = 365 nm), the fluorescence of the solution gradually changed from bright yellow to light blue, before being quenched. It is worth noting that the fluorescence changes observed at low concentration are significantly faster than those measured at high concentration. The absorption spectrum of **DCSO** showed a hypochromic blue shift at 390 nm, with a hyperchromic shift at 240 nm (Fig. 3a), while the fluorescence spectra exhibited a blue shift and decrease in intensity (Fig. 3b). This is likely due to the destruction of the long-range molecular conjugation within the DCS group of **DCSO**.

The absolute fluorescence quantum yields (Φ_F) at different concentrations and irradiation times were also measured (Fig. 3c). The Φ_F increases with an increase in concentration and decreases with an extension of irradiation time (Figs. S16 and S17 in Supporting information), which is consistent with the phenomenon mentioned above. The fluorescence lifetime (τ) at different concentrations and different times were next measured where (Tables S2 and S3 in Supporting information), as shown in Fig. 3d, τ increased from 2.72 ns to 9.04 ns as the concentration increased from 16 μmol/L to 512 μmol/L. We attempted to understand the changes in the molecular structure of **DCSO** using ^{1}H NMR, however, the signals in D_2O gave inconclusive results. We then employed high-resolution ESI-MS to examine a sample of a fluorescence-quenched solution (Figs. S12 and S13 in Supporting information), which suggested the formation of a **DCSO** dimer. Notably, intermolecular cyclodimerization is more likely to occur when cyanostilbene units exist in an aggregated state [49].

Information encryption materials have become more and more important in recent times, but examples of those encrypted on a time scale are still in the preliminary stages of development [50–54]. Given that our material has multiple responses, we tried to create a multi-functional information encryption model. As shown in Fig. 4a, by using different concentrations of solution to encode information on a core plate, emission intensity and color can be controlled on a UV irradiation time scale. As a proof-of-concept test, the messages "Y" (for "yes") and "N" (for "no") were encoded by simply using a solution with a high concentration (256 μmol/L) and a low concentration (16 μmol/L) (Fig. 4b). As a result, the information can be decrypted either by increasing the temperature or by UV exposure. At the beginning, all solutions showed bright yellow fluoro-

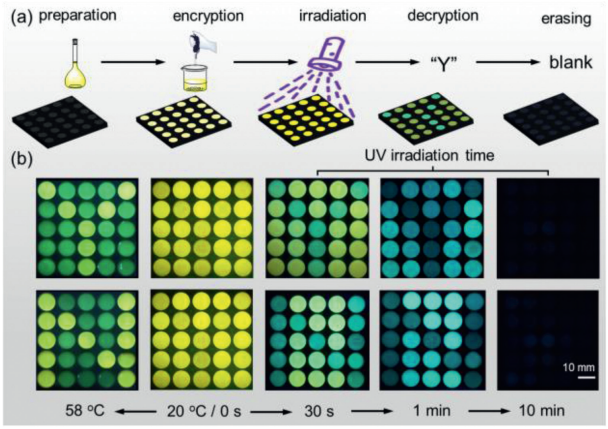

Fig. 4. Demonstration of time-dependent information encryption. (a) The steps of the information encryption process. (b) Proof-of-concept testing revealed that coded messages "Y" (for "yes") and "N" (for "no") were decoded by increasing the temperature or by UV exposure and eventually erased with prolonged exposure to UV light.

rescence was decoded and displayed as the emission color of the concentrated solutions change to green. Moreover, as the UV light irradiation time increased, the information with green fluorescence was decoded and displayed. With further extension of the irradiation time, the information was gradually erased. The message can only be read at a certain time, that is, using a "time key" to decrypt the message. The function of time encryption may allow for 'secrecy levels' of fluorescent display materials and has great potential in practical applications, such as adding time locks to doors.

In summary, we have developed a multiple stimuli-responsive system based on a single-fluorophore amphiphilic molecule **DCSO**, which can self-assemble into nanoparticles in water. Since the DCS group is AIE active and the OEG coil is thermally responsive, the material shows a blue-shift in fluorescence from yellow to green upon heating. In addition, the molecule exhibits solvatochromic and humidity-responsive fluorescence, which has the potential to indicate solvent polarity and humidity levels. On account of the intermolecular cyclodimerization of aggregated **DCSO** under UV irradiation, fluorescence studies showed concentration- and time-dependent changes in both color and intensity. Taking advantage of this, solutions of different concentrations were used to encode specific information. This information was dynamic on a short time scale, and the correct information could be decrypted under irradiation at a specific time point. In addition, the information encoded by different concentrations can also be decrypted at a specific temperature. We believe this work can serve as an inspiring basis for the creation of single-fluorophore-based smart materials with multi-responsive properties.

Declaration of competing interest

The authors declare that they have no known competing financial interests or personal relationships that could have appeared to influence the work reported in this paper.

Acknowledgments

This research work was financially supported by the National Natural Science Foundation of China (No. 21702020) and partially supported by the Starry Night Science Fund of Zhejiang University Shanghai Institute for Advanced Study (No. SN-ZJU-SIAS-006). The authors also acknowledge the analytical testing support from Analysis and Testing Center, NERC Biomass of Changzhou University. The authors also thank Shiyanjia Lab (www.shiyanjia.com) for the support of HR-MS and TEM test.

Supplementary materials

Supplementary material associated with this article can be found, in the online version, at doi:10.1016/j.cclet.2023.108617.

References

[1] G. Isapour, M. Lattuada, Adv. Mater. 30 (2018) 1707069.
[2] Y. Wang, H. Cui, Q. Zhao, et al., Matter 1 (2019) 626–638.
[3] H.H. Chou, A. Nguyen, A. Chortos, et al., Nat. Commun. 6 (2015) 8011.
[4] X. Zhang, L. Chen, K.H. Lim, et al., Adv. Mater. 31 (2019) 1804540.
[5] P. Theato, B.S. Sumerlin, R.K. O'Reilly, et al., Chem. Soc. Rev. 42 (2013) 7055–7056.
[6] S. Mura, J. Nicolas, P. Couvreur, Nat. Mater. 12 (2013) 991–1003.
[7] D. Roy, J.N. Cambre, B.S. Sumerlin, Prog. Polym. Sci. 35 (2010) 278–301.
[8] J. Zhang, B. He, Y. Hu, et al., Adv. Mater. 33 (2021) 2008071.
[9] H. Duan, F. Cao, M. Zhang, et al., Chin. Chem. Lett. 33 (2022) 2459–2463.
[10] B. Lu, S. Liu, D. Yan, Chin. Chem. Lett. 30 (2019) 1908–1922.
[11] Z. Guo, G. Li, H. Wang, et al., J. Am. Chem. Soc. 143 (2021) 9215–9221.
[12] T. Xiao, J. Wang, Y. Shen, et al., Chin. Chem. Lett. 32 (2021) 1377–1380.
[13] Z. Cao, D. Wu, M. Li, et al., Chin. Chem. Lett. 33 (2022) 1533–1536.
[14] K. Lou, Z. Hu, H. Zhang, et al., Adv. Funct. Mater. 32 (2022) 2113274.
[15] T. Chen, Y.J. Ma, D. Yan, Adv. Funct. Mater. 33 (2023) 2214962.
[16] Y.J. Ma, G. Xiao, X. Fang, et al., Angew. Chem. Int. Ed. 62 (2023) e202217054.
[17] Z. Wang, L. Gao, Y. Zheng, et al., Angew. Chem. Int. Ed. 61 (2022) e202203254.
[18] W. Luo, G. Wang, Adv. Opt. Mater. 8 (2020) 2001362.
[19] Z. Yang, Z. Chi, Z. Mao, et al., Mater. Chem. Front. 2 (2018) 861–890.
[20] J. Zhou, B. del Rosal, D. Jaque, et al., Nat. Methods 17 (2020) 967–980.
[21] M. Luo, X. Li, L. Ding, et al., Angew. Chem. Int. Ed. 59 (2020) 17018–17025.
[22] H. Xiao, P. Li, B. Tang, Coord. Chem. Rev. 427 (2021) 213582.
[23] R. Huang, C. Wang, D. Tan, et al., Angew. Chem. Int. Ed. 61 (2022) e202211106.
[24] S.H. Hwang, H. Kim, H. Ryu, et al., J. Am. Chem. Soc. 144 (2022) 1778–1785.
[25] Q. Wang, Q. Zhang, Q.W. Zhang, et al., Nat. Commun. 11 (2020) 158.
[26] P.F. Wei, T.R. Cook, X.H. Yan, et al., J. Am. Chem. Soc. 136 (2014) 15497–15500.
[27] D. Görl, B. Soberats, S. Herbst, et al., Chem. Sci. 7 (2016) 6786–6790.
[28] H.Q. Peng, B. Liu, P. Wei, et al., ACS Nano 13 (2019) 839–846.
[29] T. Xiao, L. Zhou, L. Xu, et al., Chin. Chem. Lett. 30 (2019) 271–276.
[30] Y. Cai, Z. Zhang, Y. Ding, et al., Chin. Chem. Lett. 32 (2021) 1267–1279.
[31] Q. Zhang, S. Dong, M. Zhang, et al., Aggregate 2 (2021) 35–47.
[32] T. Xiao, L. Tang, D. Ren, et al., Chem. Eur. J. 29 (2023) e202203463.
[33] T. Xiao, D. Ren, K. Diao, et al., Chem. Asian J. 17 (2022) e202200386.
[34] Q. Wang, Z. Qi, Q.M. Wang, et al., Adv. Funct. Mater. 32 (2022) 2208865.
[35] Y. Deng, X. Li, C.Y. Han, et al., Chin. Chem. Lett. 31 (2020) 3221–3224.
[36] S. Wang, Z. Xu, T. Wang, et al., Nat. Commun. 9 (2018) 1737.
[37] D. Görl, F. Würthner, Angew. Chem. Int. Ed. 55 (2016) 12094–12098.
[38] Z. Li, Z. Yang, Y. Zhang, et al., Angew. Chem. Int. Ed. 61 (2022) e202206144.
[39] T. Dünnebacke, K.K. Kartha, J.M. Wahl, et al., Chem. Sci. 11 (2020) 10405–10413.
[40] L. Ascherl, E.W. Evans, M. Hennemann, et al., Nat. Commun. 9 (2018) 3802.
[41] Z.Z. Lu, R. Zhang, Y.Z. Li, et al., J. Am. Chem. Soc. 133 (2011) 4172–4174.
[42] J.H. Kim, T. Schembri, D. Bialas, et al., Adv. Mater. 34 (2022) e2104678.
[43] X. Yang, S. Liu, Dyes Pigm. 159 (2018) 331–336.
[44] K. Cai, J. Xie, D. Zhao, J. Am. Chem. Soc. 136 (2014) 28–31.
[45] J.L. Belmonte-Vázquez, Y.A. Amador-Sánchez, L.A. Rodríguez-Cortés, et al., Chem. Mater. 33 (2021) 7160–7184.
[46] L.A. Rodríguez-Cortés, A. Navarro-Huerta, B. Rodríguez-Molina, Matter 4 (2021) 2622–2624.
[47] Y. Xue, S. Jiang, H. Zhong, et al., Angew. Chem. Int. Ed. 61 (2022) e202110766.
[48] S.K. Bhaumik, S. Banerjee, ACS Appl. Mater. Interfaces 14 (2022) 36936–36946.
[49] P. Wei, J.X. Zhang, Z. Zhao, et al., J. Am. Chem. Soc. 140 (2018) 1966–1975.
[50] Y. Zhang, X. Zhang, Z. Feng, et al., ACS Appl. Mater. Interfaces 13 (2021) 44797–44805.
[51] Z. Zong, Q. Zhang, D.H. Qu, Chem. Eur. J. 28 (2022) e202202462.
[52] S. Liu, Y. Lin, D. Yan, Sci. Bull. 67 (2022) 2076–2084.
[53] F. Nie, B. Zhou, K.Z. Wang, et al., Chem. Eng. J. 430 (2022) 133084.
[54] F. Nie, K.Z. Wang, D. Yan, Nat. Commun. 14 (2023) 1654.